Pharmaceutical Research, Vol. 27, No. 1, January 2010 (© 2009)
DOI: 10.1007/s11095-009-0005-1

Research Paper

The Targeting Behavior of Folate-Nanohydrogel Evaluated by Near Infrared Imaging System in Tumor-Bearing Mouse Model

Jian Zhang,[1] Dawei Deng,[1] Zhiyu Qian,[2] Fei Liu,[1] Xinyang Chen,[1] Lianxiao An,[1] and Yueqing Gu[1,3]

Received July 30 2009; accepted October 27 2009; published online November 11, 2009

Purpose. To synthesize P[(Folate-Allylamine)-co-(N-isopropylacrylamine)- co-Acrylamide] (P(FoAAn-co-NIPA-AAm), folate-NHG) with appropriate diameter and lower critical solution temperature (LCST) for targeting to folate receptor (FR) expressing tumors.
Methods. Folate-NHG was synthesized by free-radical precipitation polymerization method reported in our previous work and other reports. LCST, diameter and morphology of folate-NHG were characterized by UV-vis spectrophotometer, laser particle size analyzer (LPSA) and transmission electron microscope (TEM), respectively. No.12 near infrared dye (NIRD-12) was entrapped into folate-NHG by hydrophobic association to trace the *in vivo* dynamic behavior of folate-NHG. This process was evaluated by a homemade near infrared (NIR) imaging system.
Results. Spherical folate-NHG with diameter of about 50 nm and LCST of about 40°C was successfully synthesized. The photo stability of NIRD-12 was strengthened after being entrapped into folate-NHG, which enabled NIRD-12 to better trace the *in vivo* dynamic process of folate-NHG. Folate-NHG showed good targeting capability for all three folate receptor expressing tumor models (SMMC-7721, Bel-7402 and HeLa) with different sizes, and this accumulation could last for more than 96 h. D-folate-NHG, synthesized with double amount of FoAAn, showed better targeting effect for SMMC-7721 tumor model than that of folate-NHG.
Conclusions. Folate-NHG could actively accumulate in three models of folate receptor positive tumors with different sizes and keep retention for more than 96 h, which enables it to be used as a diagnostic reagent or anti-tumor drug carrier for tumor therapy.

KEY WORDS: active targeting; folate receptor; nanohydrogel; NIR imaging; tumor.

INTRODUCTION

The incidence of malignant tumors has increased rapidly over the past decade, resulting in the extensive utilization of many kinds of cytotoxic drugs. However, conventional administered anti-tumor drugs have shortcomings, such as severe side effects and poor therapeutic activity. Furthermore, most cytotoxic drugs, hydrophilic or hydrophobic, are micro-molecules and have no controlled- and sustained-release properties. As a result, frequent administration is used to keep adequate blood drug level for persistent tumor inhibition. This results in the unsteady blood concentration and decreases the compliance of cancer patients. To overcome these disadvantages, targeted drug delivery systems that deliver chemotherapeutics specifically to a region of interest (ROI) have been developed (1–6). Among these strategies, one approach, having received extensive attention, is the use of folic acid to deliver attached drugs/macromolecular carriers selectively to folate receptor (FR) positive cancer cells (7–13).

Folic acid (folate) is required in single carbon metabolic reactions, and, consequently, is essential for the synthesis of nucleotide bases. FR, known as the folate binding protein (FBP) with a naturally 38-kDa glycopolypetide, is over-expressed in many cancer cells, including cancers of the ovary, kidney, uterus, testis, brain, colon and lung (14). Folate

[1] Department of Biomedical Engineering, School of Life Science and Technology, China Pharmaceutical University, Tongjia Lane No. 24, Nanjing 210009, People's Republic of China.
[2] Department of Biomedical Engineering, School of Automation, Nanjing University of Aeronautics and Astronauticss, Nanjing 210016, People's Republic of China.
[3] To whom correspondence should be addressed. (e-mail: guyueqing@hotmail.com)

ABBREVIATIONS: AAm, Acrylamide; AAn, Allylamine; BIS, N,N-methylene-bis-acrylamide; CCD, charge-coupled device; CT, computed tomography; DCC, N, N'-Dicyclohexylcarbodiimide; DCU, dicyclohexylurea; D-folate-NHG, special folate-NHG synthesized with as double amount of FoAAn as that of folate-NHG; DMSO, dimethyl sulfoxide; FBP, folate binding protein; FoAAn, folate-Allylamine; folate-NHG or P(FoAAn-co-NIPA-co-AAm), P[(Folate-Allylamine)-co-(N-isopropylacrylamide)-co-Acrylamide]; FR, folate receptor; KPS, Potassium persulfate; LC, loading content; LC-MS, liquid chromatograph-mass spectrum; LCST, lower critical solution temperature; LPSA, laser particle size analyzer; MR, magnetic resonance; MTT, methyl thiazolyl tetrazolium; NHG, nanohydrogel; NHS, N-hydroxysuccinimide; NIPA, N-isopropylacryl-amide; NIR, near infrared; NIRD-12, No.12 near infrared dye; non-NHG, P[(N-isopropylacrylamide)-co-Acrylamide]; PNIPA, P(N-isopropylacrylamide); ROI, region of interest; RPMI, Roswell Park Memorial Institute; RT, room temperature; SBF, simulated body fluid; SDS, sodiumdodecyl sulfate; TEA, triethanolamine; TEM, transmission electron microscope; US, ultrasonography; Wt%, $((W_{AAm}/W_{NIPA})\times 100\%)$.

and folate conjugates bind to FR with high affinity (Kd ~ 10^{-9}M) and enter FR-expressing cells by receptor-mediated endocytosis (8,14). Since the FR-mediated endocytosis was first discovered by Philip S. Low and Christopher P. Leamon in Purdue University in 1991, folate has been widely used as an optimal targeting ligand for selective delivery of attached drugs or macromolecular carriers to tumors (15). More and more folate conjugations have been developed and used in tumor treatment and imaging, such as polymeric carriers (10–12) and small imaging or therapeutic agents (16–21). At least four folate-conjugated drugs/prodrugs (^{111}In-DTPA-folate, EC17, EC20 and EC145), designed by Philip S. Low and Christopher P. Leamon, have entered human clinical trials (22).

Generally, a relatively complicated route was needed for preparing a folate-conjugated prodrug (22), and this kind of prodrug had no property of sustained release. The conjugation of folate and drug-loaded polymeric carrier was a promising way to overcome this shortcoming. Drug-loaded folate-polymers have several advantages (23): (1) an increase in water solubility and bioavailability of insoluble drugs; (2) protection of drug from deactivation and preservation of its activity during circulation, transport to targeted organ or tissue and intracellular trafficking; (3) an improvement in pharmacokinetics; (4) the ability to provide passive/active targeting of the drug. Among these polymeric carriers, N-isopropylacrylamide (NIPA)-based polymers have drawn more and more attention owing to their intelligently responsive property and low cytotoxicity (24,25). They have been extensively studied in gene delivery (26–29), controlled drug delivery system (30–33) and thermally targeted study (34–37). But few reports adressed the combination of folate targeting capability and the intelligently responsive property of NIPA-based polymers. Based on these considerations, P((folate-allylaine)-co-NIPA-co-Acrylamide) (P(FoAAn-co-NIPA-co-AAm), or folate-NHG), the conjugate of folate and NIPA-based NHG, was synthesized for active targeting of FR overexperessed tumor.

Compared to tumor therapy, the early detection of tumors sometimes could be a more important measure to reduce the mortality of tumor patients. Current routines for tumor assessments are largely based upon structural change, such as computed tomography (CT) (38) and magnetic resonance (MR) (39). However, the precondition for tumor detection with these techniques is that their relative volume must be bulky enough, which hinders the early diagnosis of malignant tumors and results in high mortality. Optical imaging, especially near infrared (NIR) fluorescence imaging, may have advantages over the existing techniques for early diagnosis of tumors. It possesses many advantages as a non-invasive technique for *in vivo* real-time monitoring or tracing of biological information and signals in living subjects (40,41). The wavelength range of NIR light (NIR) is from 700 to 900 nm, avoiding the high absorption of intrinsic chromospheres, such as hemoglobin and water and, thus, penetrating relatively deep tissue. NIRD-12, a kind of hydrophobic dye (2~3 μg/ml in water) with maximum absorption at 772 nm and emission peak at 814 nm, was chosen for the *in vivo* tracer of folate-NHG. It was entrapped into folate-NHG by hydrophobic association effect (37). After entrapment, the photo stability of NIRD-12 was obviously enhanced, which made it more suitable for *in vivo* imaging experiment. Injection of NIRD-12-loaded folate-NHG could effectively avoid the false positive result of tumor diagnosis on account of two facts: (1) Free NIRD-12 could be rapidly cleared out from blood circulation because of its poor water-solubility; (2) NIRD-12-loaded folate-NHG had property of low leakage because of the strong binding force between them (37).

The cytotoxicity of NIRD-12-loaded folate-NHG was estimated by MTT assay of Human Vein Endothelial Cell Line (EVC304). The tumor targeting capability of folate-NHG was determined *in vivo* in athymic nude mice bearing different tumor xenografts (SMMC-7721, Bel-7402, HeLa) with different sizes by using the NIR fluorescence imaging system. This paper focuses on the synthesis, characterization, and *in vivo* targeting behavior of folate-NHG. Future work would include researching *in vitro* release profiles and anti-tumor efficacy of drug-loaded folate-NHG.

MATERIALS AND METHODS

Materials

Folic acid (folate, MW 441), N,N'-Dicyclohexylcarbodiimide (DCC) and N-hydroxysuccinimide (NHS) were all purchased from Sigma-Aldrich (Shanghai, China). N-isopropylacrylamide (NIPA, ≥99% in purity), Acrylamide (AAm), Allylamine (AAn) and N,N-methylene-bis-acrylamide (BIS) were all purchased from Aldrich-Chemie (Steinheim, Germany) and used without further purification. Potassium persulfate (KPS) and sodiumdodecyl sulfate (SDS) were both supplied by Huakang Technology Company (Jiangsu, China). No. 12 near infrared dye (NIRD-12) was obtained from Huahai Lanfan Chemical Technology Company (Liaoning, China). Methyl thiazolyl tetrazolium (MTT) and other reagents for cell cultivation were all purchased from Gibco (Life Technologies, Shanghai, China). Triethanolamine (TEA), dimethyl sulfoxideand (DMSO) and other chemical solvents used in this study were all acquired from Shanghai Chemical Company with analytical reagent grade (Shanghai, China). Water for all reactions, solution preparation and sample purification was double distilled.

NIR Fluorescence Imaging System

A self-built NIR imaging system, real-time and non-invasive, was used to evaluate the *in vivo* targeting behavior of folate-NHG. This NIR imaging system has been introduced in detail in our previous work (24,36), and schematic diagram of this system was shown in Fig. 1.

Synthesis of Folate-NHG

The synthesis of folate-NHG contained two steps: (1) the conjugation of folate and AAn; (2) the copolymerization of folate-Allylamine (FoAAn), NIPA and AAm (Fig. 2).

In this study, FoAAn was synthesized following a protocol reported by Destito's group (42). In this protocol, DCC (310 mg)/NHS (230 mg) system was employed for the conjugation of folic acid (440 mg) and AAn (230 mg) in anhydrous DMSO (Fig. 2). After conjugation, the ultimate mixture was precipitated by acetone. The precipitation was then dried and identified by liquid chromatograph-mass spectrum (LC-MS) (Agilent 1100 Series LC/MSD Trapmass

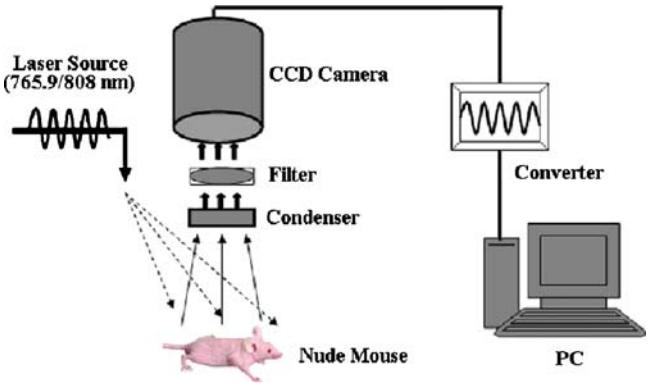

Fig. 1. Schematic diagram of NIR fluorescence imaging system.

spectrum, Shanghai, China) and UV-vis spectrophotography (JH 754PC, Shanghai, China).

A series of folate-NHGs with different feed compositions (Table I) were synthesized by free-radical precipitation polymerization reported in our previous work (36,37). The resultant NHGs were cooled down to RT and then dialyzed (MW cut off 10 kDa) against double-distilled water for 5 days. The dialyzed aqueous solutions of NHGs were then lyophilized to obtain dried powder for subsequent research.

NHG10 was named as D-folate-NHG for being synthesized with a double amount of FoAAn as that of folate-NHG. NHG11 was named as non-NHG for having no folate in its backbone.

Characterization of Folate-NHG

LCST Determination of Folate-NHG in Hanks Simulated Body Fluid (SBF)

Optical transmittance of folate-NHGs (NHG1-5, 5 mg/ml) in Hanks SBF (Table II) at various temperatures was measured at 500 nm with UV-vis spectrophotography. Wt%

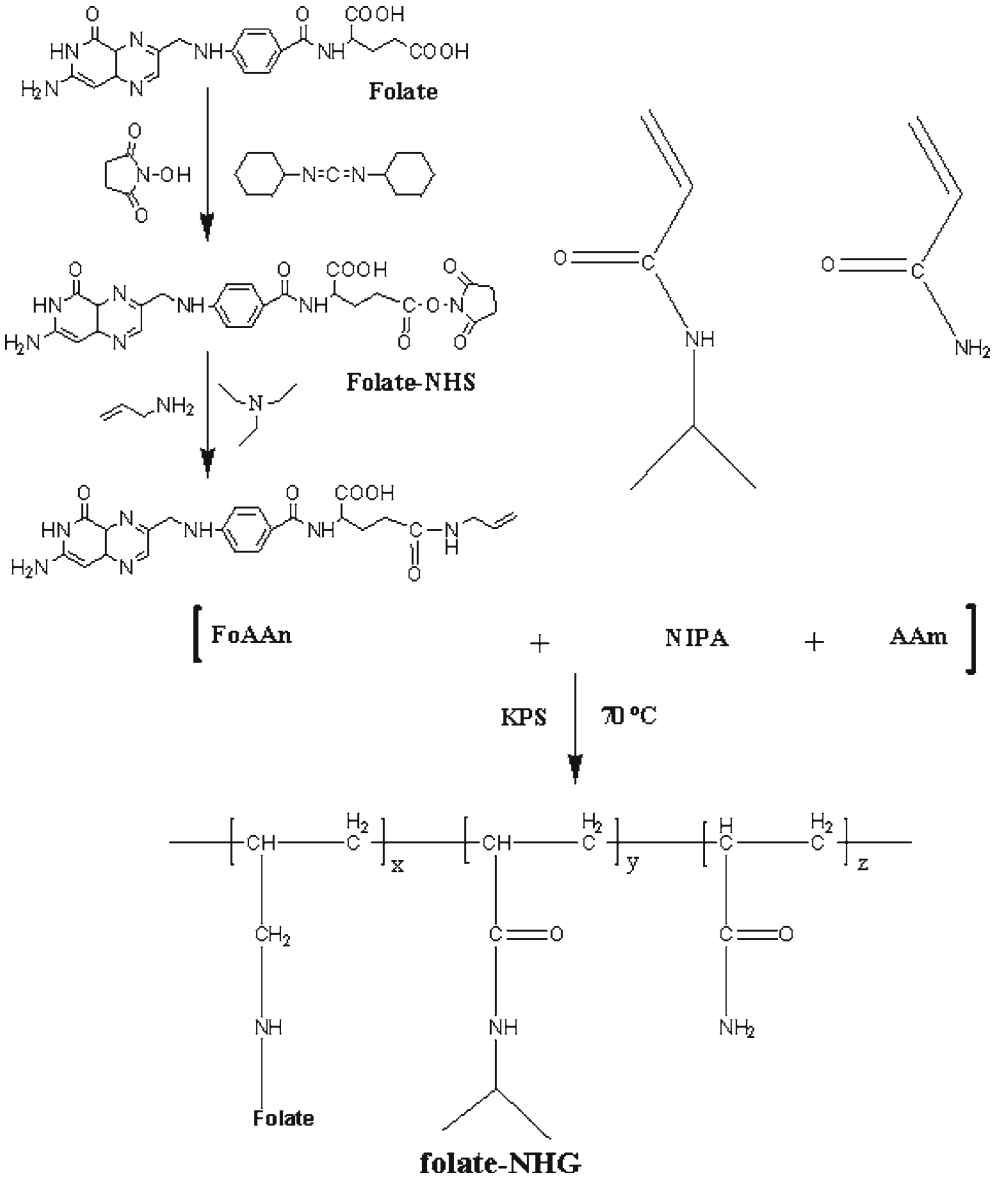

Fig. 2. Synthesis of folate-Allylamine (FoAAn) and folate-NHG.

Table I. Feed Compositions of the Folate-NHG

Samples	FoAAn (mg)	NIPA (mg)	AAm (mg)	BIS (mg)	SDS (mg)	KPS (mg)	H_2O (mL)
NHG1	50	1000	50	27	200	75	100
NHG2	50	1000	100	27	200	75	100
NHG3	50	1000	150	27	200	75	100
NHG4	50	1000	200	27	200	75	100
NHG5	50	1000	250	27	200	75	100
NHG6	50	1000	200	27	150	75	100
NHG7	50	1000	200	27	100	75	100
NHG8	50	1000	200	27	75	75	100
NHG9	50	1000	200	27	50	75	100
NHG10	100	1000	250	27	200	75	100
NHG11	0	1000	200	27	200	75	100

NHG10 was named as D-folate-NHG for being synthesized with a double amount of FoAAn as that of folate-NHG. NHG11 was named as non-NHG for having no folate in its backbone. (n=3 for each group)

($(W_{AAm}/W_{NIPA})\times 100\%$) of NHG1–5 were 5%, 10%, 15%, 20% and 25%, respectively. Samples were thermostated by putting the cells in a waterbath with temperature changing from 30°C to 50°C. At least 10 min were allowed for each of the samples to reach equilibrium temperature. LCST of folate-NHG was defined as the temperature producing 50% decrease in optical transmittance.

Diameter and Morphology Measurement of Nanohydrogel

The average diameter and distribution of folate-NHGs (NHG4, 6–9, 5 mg/ml) were measured by Mastersizer 2000 Laser Particle Size Analyzer (LPSA, Malvern, British). Transmittance electron microscope (TEM, Philips FEI Tecnai G2 20s-TWIN) pictures of NHG4 were taken with accelerated voltage of 200 kV.

Physical Labeling of Folate-NHG with NIRD-12

NIRD-12 (0.5 mg), a kind of hydrophobic derivative of indocyanine green with maximum absorption at 772 nm and emission peak at 814 nm, was first dissolved in 10 ml of acetone and then dropwisely added to 10 ml of folate-NHG Hanks SBF (5 mg/ml). After that, the flask containing the mixture was put into dark environment and kept the beak open with constant agitation at RT for 36 h to allow the evaporation of acetone. After incubation, centrifugalization (12000 r.p.m×10 min, High speed centrifuge model 1612-1, Shanghai, China) was carried out to remove the unloaded NIRD-12. The loading content (LC) of nanohydrogel for NIRD-12 could be calculated by the following equation: $LC = \left[W_{Entrapped\ NIRD-12} / \left(W_{folate-NHG} + W_{Entrapped\ NIRD-12}\right)\right] \times 100\%$, where $W_{Entrapped\ NIRD\text{-}12}$ was obtained by the calibration curve of NIRD-12. The diameter and LCST of NIRD-12-loaded folate-NHG were also determined.

Optical Characterization of Free NIRD-12 and NIRD-12-Loaded Folate-NHG

Optical characterization of NIRD-12 and NIRD-12-loaded folate-NHG was carried out in this study according to a similar protocol reported in our previous work (37). In detail, absorbance and fluorescence spectra of free NIRD-12 and NIRD-12-loaded folate-NHG were measured by UV-vis spectrophotography and S2000 spectrometer (Ocean Optics, USA), respectively. A NL-FC-2.0-763 semiconductor laser (λ=765.9 nm, Enlight, China) was used as the excitation source of NIRD-12. The photo stability of free NIRD-12 and NIRD-12-loaded folate-NHG was evaluated by measuring their relative fluorescence intensity under continuous exposure to the laser for 2 h, with 5 min interval for data acquisition.

MTT Assay of NIRD-12-loaded Folate-NHG

MTT assay was conducted following the standard protocol reported previously (43,44) and in our previous work (36). Human Vein Endothelial Cell Line (ECV304) was chosen as the target cells. Briefly 200 μl of ECV304 in RPMI 1640 (2.0×10^5 cells/ml) was added into each well in a 96-well plate and incubated for 24 h in humidified atmosphere containing 5% CO_2 at 37.0°C. The culture medium in each well was replaced by 200 μl of RPMI 1640 containing NIRD-12-loaded folate-NHG nanohydrogel (NHG4) with particular concentrations (0 mg/ml, 0.02 mg/ml, 0.1 mg/ml, 0.2 mg/ml, 0.5 mg/ml, 1 mg/ml, 2 mg/ml). Medium without NIRD-12-loaded NHG4 was used here as control. The mixture was further incubated for 44 h. RPMI 1640 with NIRD-12-loaded NHG4 was replaced by 180 μl of fresh RPMI 1640 and 20 μl of MTT PBS solution (5 mg/ml, pH 7.4). After incubation for another 4 h, the medium containing MTT was removed from each well, and 150 μl of DMSO was added and shaken at RT. The absorbance (A) of the solution in each well was measured at 570 and 630 nm with a Microplate Reader (Biorad, USA). The viable rate could be calculated by the following equation: $\text{Viable Rate} = A_{treated} / A_{control} \times 100\%$, where $A_{treated}$ was obtained in the presence of NIRD-12-loaded

Table II. Chemical Composition of Hank SBF (m mol/L)

Na^+	K^+	Ca^{2+}	Mg^{2+}	Cl^-	HCO_3^-	HPO_4^{2-}	SO_4^{2-}
142	5	2.5	1.5	147.8	4.2	1	0.5

folate-NHG, and $A_{control}$ was obtained in the absence of NIRD-12-loaded folate-NHG.

In Vivo Targeting Behavior of Folate-NHG Evaluated by NIR Imaging System

Animal Models

The athymic nude mice (nu/nu, half male and half female) used in this study, which were 4–6 weeks old and weighed at about 18–22 g, were purchased from Charles River Laboratories (Shanghai, China). They were housed five per cage and fed with sterilized pellet chow and sterilized water. Mice were anesthetized in an isoflurane chamber before being injected subcutaneously in the right armpit with 3×10^6 tumor cells (HeLa, Bel-7402 and SMMC-7721, respectively) suspended in 50 μl sterile PBS. One to four weeks after inoculation, when the tumors reached 30–900 mm^3 in volume, the mice were used for *in vivo* imaging studies.

All experiments were carried out in compliance with the Animal Management Rules of the Ministry of Health of the People's Republic of China (document no. 55, 2001), the guidelines for the Care and Use of Laboratory Animals of China Pharmaceutical University and Principles of Laboratory Animal Care (NIH publication #85–23, revised in 1985).

In Vivo Fluorescence Imaging

Thirty athymic nude mice were evenly and randomly divided into six groups. Each mouse in each group was anesthetized with an intraperitoneal injection of 1 mg/g of ethyl carbamate and immobilized in a Lucite jig before *in vivo* fluorescence imaging. Mice of all groups were treated by systemic administration. The specific program was described in detail in Table III. The dynamic behavior of folate-NHG was monitored by the above-mentioned self-built NIR imaging system (Fig. 1.). The subjected mouse was first anesthetized and imaged at predetermined intervals (1 min, 2 h, 12 h, 24 h and 96 h) post-injection. All fluorescence images were acquired with one-second exposure (f/stop=4).

RESULTS

Synthesis and Identification of FoAAn and Folate-NHG

DCC/NHS catalytic system was used for the conjugation of folate and AAn. FoAAn could be purified by acetone according to the solubility difference of FoAAn and folate in this solvent system. The absorption spectrum and mass spectrum of FoAAn were shown in Fig. 3 (A and B). FoAAn had similar absorption spectrum with folate (Fig. 3A) because they had the same chromophores. The results of mass spectrum (m/z=479 $[M-1]^-$) also proved that the conjugate was equal to the theoretic molecular weight with FoAAn. After polymerization, the absorption spectrum of P(NIPA-co-AAm) and folate-NHG were also measured and shown in Fig. 3C. Folate-NHG had both the end absorption of P (NIPA-co-AAm) and the characteristic absorption peaks of folate (280 nm and 362 nm), which proved that the resultant polymer was folate-NHG.

Characterization of Folate-NHG

LCST, diameter and morphology are very important parameters of folate-NHG. For *in vivo* application, LCST of folate-NHG in Hanks SBF should be above 38°C. The results of our previous work (36) showed that LCST of PNIPA was around 32°C. Because of the better hydrophilicity of AAm than that of NIPA, AAm was used here to promote LCST of folate-NHG. Fig. 4A displayed the profiles of the transmittance of different folate-NHGs as a function of temperature (n=3). LCST for folate-NHG (NHG1–5) was 31.5°C, 33°C, 36°C, 40°C and 45°C, respectively. The results indicated that LCST of folate-NHG was up-regulated with the increase of Wt%, as shown in Fig. 4B (n=3).

Fig. 5A (n=3) showed the diameters of nanohydrogels (NHG4, 6–9) as a function of the concentrations of SDS. When the concentration of SDS was 0.5 mg/ml (NHG9), folate-NHG with a diameter of about 430 nm was obtained. When the concentration of SDS increased to 2 mg/ml (NHG4), the diameter of resulting folate-NHG decreased to about 50 nm (54.63±4.26 nm, mean ± SD). Fig. 5 (B and C) showed that folate-NHG particles were spherical and had good diameter distribution. The results of SDS concentration towards the modulation of polymer diameters were consistent with our previous work (36,37).

Physical Labeling of Folate-NHG with NIRD-12

NIRD-12 is an extremely hydrophobic dye with maximum absorbance at 772 nm and maximum emission at 814 nm. It could be easily entrapped into folate-NHG by hydrophobic association effect. The LC and entrapment rate of folate-NHG for NIRD-12 were 1.02% (w/w) and 102%, respectively. LCST and diameter of the dye-loaded folate-NHG have no apparent change before and after physical labeling with NIRD-12 (data not shown here). Red shifts of

Table III. Experimental Scheme for *In Vivo* Fluorescence Imaging Test

Group	A	B	C	D	E	F
Tumor model	SMMC-7721	SMMC-7721	SMMC-7721	SMMC-7721	HeLa	Bel-7402
Tumor volume (mm^3)	200–400	200–400	200–400	200–400	30–60	600–900
Injectant	NIRD-12	NHG	Folate-NHG	D-folate-NHG	Folate-NHG	Folate-NHG
Dose (μg)	5	5	5	5	5	5

Dose for each group was calculated by the amount of NIRD-12.

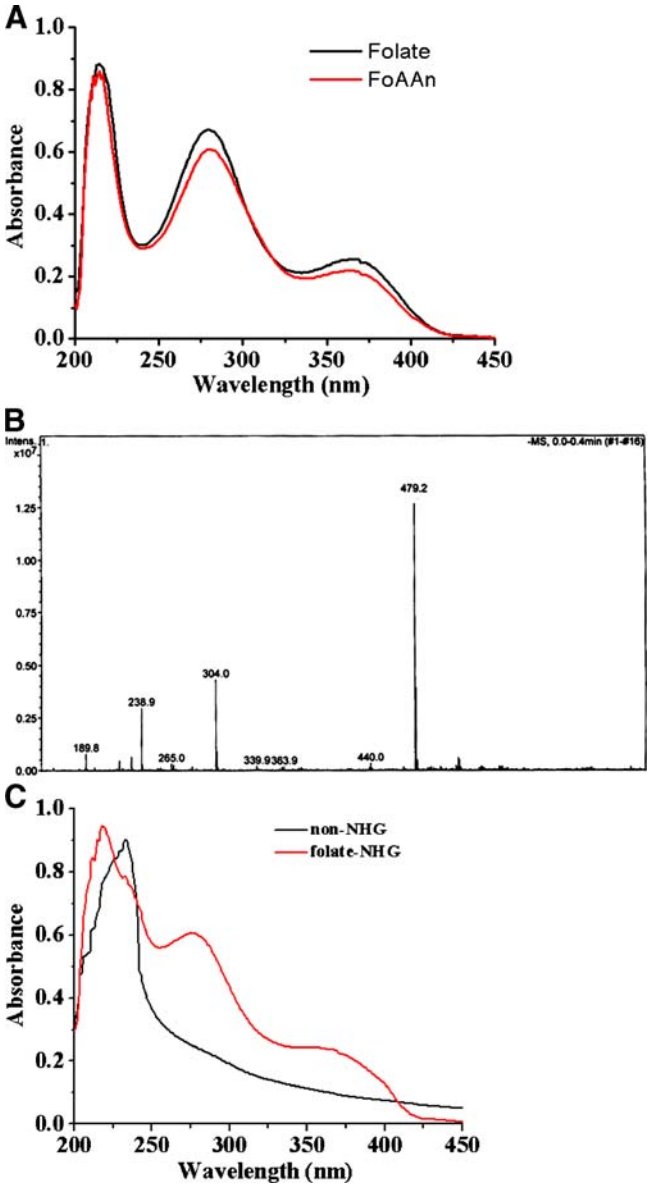

Fig. 3. Identification of FoAAn and folate-NHG with UV-vis spectrophotography and LC-MS: **A** Absorbance of folate and FoAAn as a function of wavelength; **B** Primary mass spectrum of folate-NHG; **C** Absorbance of non-NHG and folate-NHG.

both absorbance and fluorescence spectra of NIRD-12 were observed (Fig. 6A and B) after the process of entrapment. The photo stability of NIRD-12 was also significantly enhanced after being entrapped by folate-NHG (Fig. 6C). The enhancement of the NIRD-12's photo stability made it more suitable to trace the dynamic process of folate-NHG in mouse model evaluated by the self-built NIR imaging system.

Cytotoxicity of Folate-NHG

MTT assay was carried out to evaluate the cytotoxicity of NIRD-12-loaded folate-NHG (NHG4) on the ECV304 cells. The inhibition of NIRD-12-loaded NHG4 on the proliferation of ECV304 was studied and no apparent cytotoxicity was observed (Fig. 7, $n=6$).

In Vivo Folate-Receptor Mediated Targeting Test

Folate-NHG (NHG4) with diameter of about 50 nm and LCST of about 40°C was chosen for *in vivo* FR mediated targeting test. Fig. 8 shows the *in vivo* dynamic processes of NIRD-12-loaded folate-NHG and corresponding blank samples in athymic nude mice evaluated by NIR fluorescence imaging system. Images of group A (Fig. 8, control group) showed that free NIRD-12 had no targeting effect toward SMMC-7721 tumor cells. Images of group B (Fig. A, the other control group) indicated that non-NHG, without the help of folate, had slightly targeted retention in tumor tissue at 24 h post-injection. The passively targeted behavior of non-NHG for SMMC-7721 tumor was due to the ERP (Enhanced Retention and Penetration) effect, which was caused by the leakage property of tumor tissue.

For group C, folate-NHG had apparent accumulation in SMMC-7721 tumor tissue at 2 h post-injection. The fluorescence intensity in ROI persistently enhanced and reached the maximum at 24 h post-injection. Strong fluorescence was observed even at 96 h post-injection. Images of group D (Fig. 8) showed that D-folate-NHG had better tumor targeting capability than that of folate-NHG, and fluorescence intensity in ROI reached the maximum at 12 h post-injection. Fluorescence intensity in ROI of group D was slightly stronger than that of group C at 2 h, 12 h and 24 h post-injection. Apparent fluorescence in ROI was also observed at 96 h post-injection for mice of group D. Targeting capability

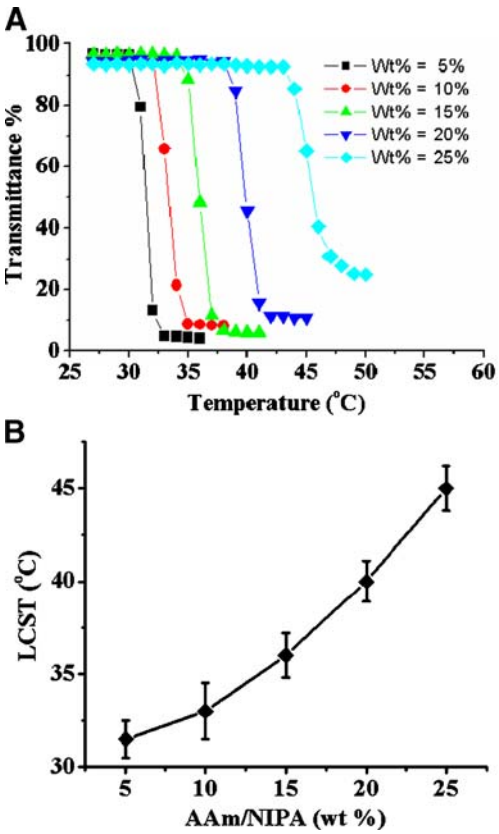

Fig. 4. **A** Transmittance% of folate-NHG with different Wt% as a function of temperature ($n=3$); **B** LCST of folate-NHG in Hanks SBF as a function of Wt% ($n=3$). ($Wt\% = (W_{AAM}/W_{NIPA}) \times 100\%$).

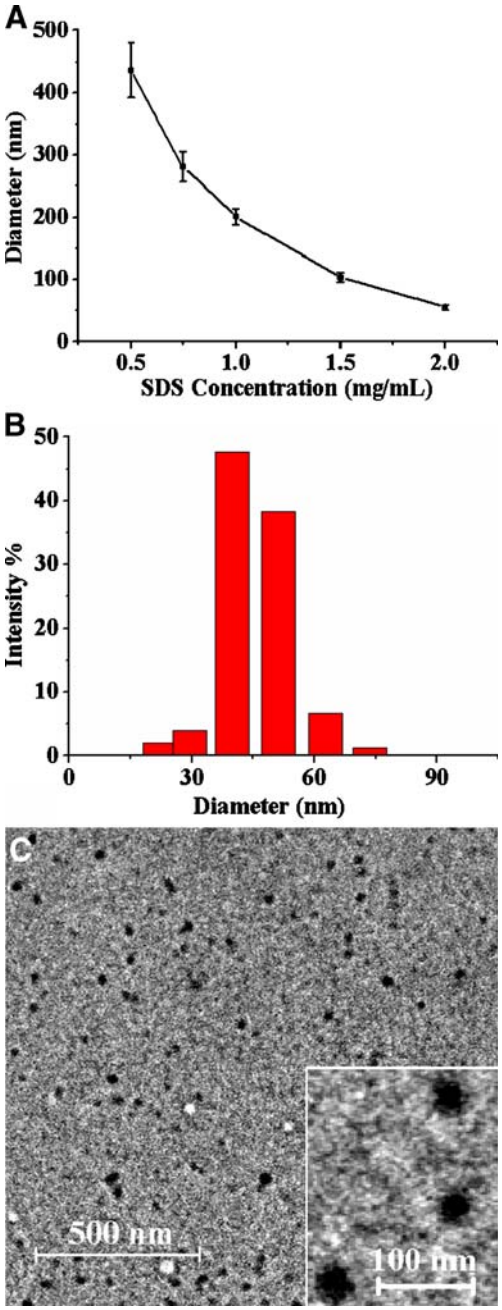

Fig. 5. **A** Diameter of folate-NHG as a function of SDS concentration (n=3); **B** Size distribution of folate-NHG (NHG4) at 25°C; **C** Transmittance electron microscope (TEM) pictures of folate-NHG (NHG4).

of folate-NHG for HeLa-bearing mice (tiny tumor, 30–60 mm^3) and Bel-7402-bearing mice (large tumor, 30–60 mm^3) was also investigated. Results showed that folate-NHG could obviously accumulate in both little HeLa tumor and big Bel-7402 tumor at 12 h post-injection. This accumulation reached the maximum at 24 h post-injection and clear fluorescence signals were also detected at 96 h post-injection.

Control tests for groups E and F were also carried out according to the same procedure for SMMC-7721-bearing mouse model, and similar results were received (images not shown here).

DISCUSSION

The first experimental route for the synthesis of folate-NHG was (1) polymerization of "P(AAn-co-NIPA-co-AAm)" with AAn, NIPA and AAm; (2) conjugation of folate and "P(AAn-co-NIPA-co-AAm)." But in fact, AAn had extremely low polymerization ratio in aqueous system, and the preparation of "P(AAn-co-NIPA-co-AAm)" was difficult, as proved in our experiment. The specific mechanism of this phenomenon was not clear. It may have been caused by the inactivation of the amino groups of AAn towards the free radicals. Therefore, for the success of synthesis of folate-NHG in this polymerization system, the first step should be the conjugation of folate and AAn, and the second step should be the polymerization process.

As to the characterization of folate-NHG, only UV absorption does not suffice the formation of folate-NHG if

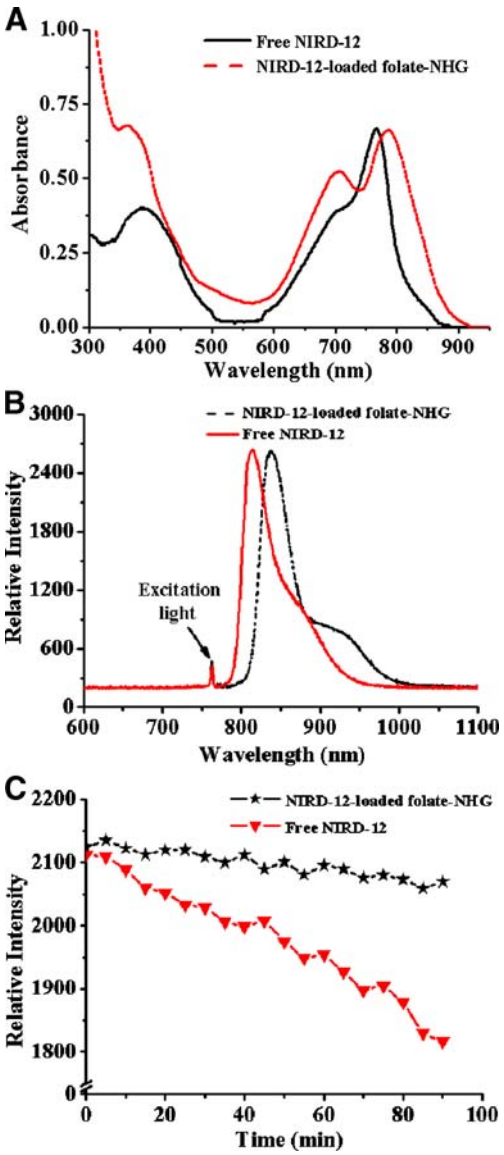

Fig. 6. Optical characterization of free NIRD-12 and NIRD-12-loaded folate-NHG: **A** Absorbance spectra; **B** Fluorescence spectra; **C** Photo stability.

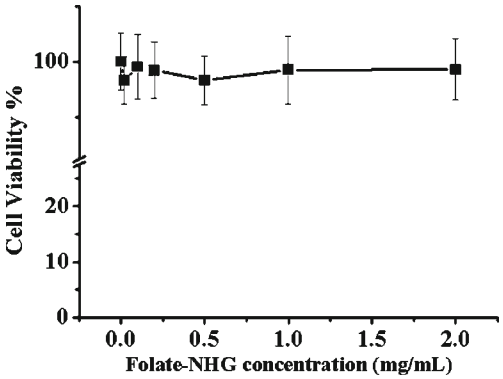

Fig. 7. MTT assay of folate-NHG (mean±SD, n=6).

we focused on the synthesis process. Although the synthesis of nanohydrogel is a matured technique and several papers had been reported by our group, it is difficult to directly determine the exact composition of folate-NHG because of the lack of quantitative parameters, such as characteristic absorption, nuclides or unique element. Some studies and our previous papers reported the characterization of the polymer particle by IR spectrum. Actually, IR spectrum only indicates the existence of some specific bonds, rather than the exact particle composition, and UV absorption could just display the unique groups in the particle. Even so, the results of *in vivo* targeting test may prove in turn that folate-NHG was successfully synthesized in this study. And the emphasis of this study was placed on *in vivo* application of folate-NHG. Therefore, loading content and targeting capability of folate-NHG are much more important parameters for its *in vivo* application.

LCST is a key parameter of folate-NHG. Folate-NHG particles could keep in a state of swelling under LCST because of the hydrogen bond interaction between folate-NHG particles and water molecules. According to our previous work, PNIPA NHG has LCST of about 32°C, lower than physiological temperature. FoAAn was a hydrophobic monomer, which will further decrease LCST of NHG, so a more hydrophilic monomer was necessary for the synthesis of folate-NHG with higher LCST than physiological temperature. The hydrophilicity of AAm is better than that of NIPA. The more hydrophilic moiety of AAm in folate-NHG, the stronger hydrogen bond interaction it produces. The resultant interaction requires more energy to destroy it, resulting in the increase of LCST. Thus, LCST of NHG could be adjusted by modulating Wt%.

Diameter is another important parameter of folate-NHG, and SDS is a popular anionic detergent to be used to regulate the size of folate-NHG according to the mechanism of electrostatic repulsion, which was confirmed in our previous work and other reports (36,37,45,46). Electrostatic repulsion force between the polymer chains in the process of polymerization was strengthened accordingly with the increase of SDS concentration, which resulted in the shorter chain of the polymer, and thus, the smaller particle size. For *in vivo* application, folate-NHG particles should have appropriate diameters: larger particles have stronger immunogenicity and smaller particles have worse LC. Folate-NHG with diameter of about 50 nm was proved to be appropriate in our previous work (36,37), which calls for the concentration of SDS up to 2 mg/ml. Due to the inherent toxicity, N-lauroylsarcosine sodium salt, a kind of anionic surfactant with low toxicity and pungency, was once chosen to replace SDS. Unluckily, N-lauroylsarcosine sodium salt was not appropriate to this polymerization system for its unfavorable foaming characteristics. As a result, we came back to SDS and made efforts to lower the residual level of SDS. The result of element analysis of sulfur showed that SDS was successfully removed (data now shown here), and the resultant folate-NHG samples did not show apparent cytotoxicity in the MTT assay.

From Fig. 5 (A and C), average diameter of folate-NHG particles determined by LPSA was slightly larger than that

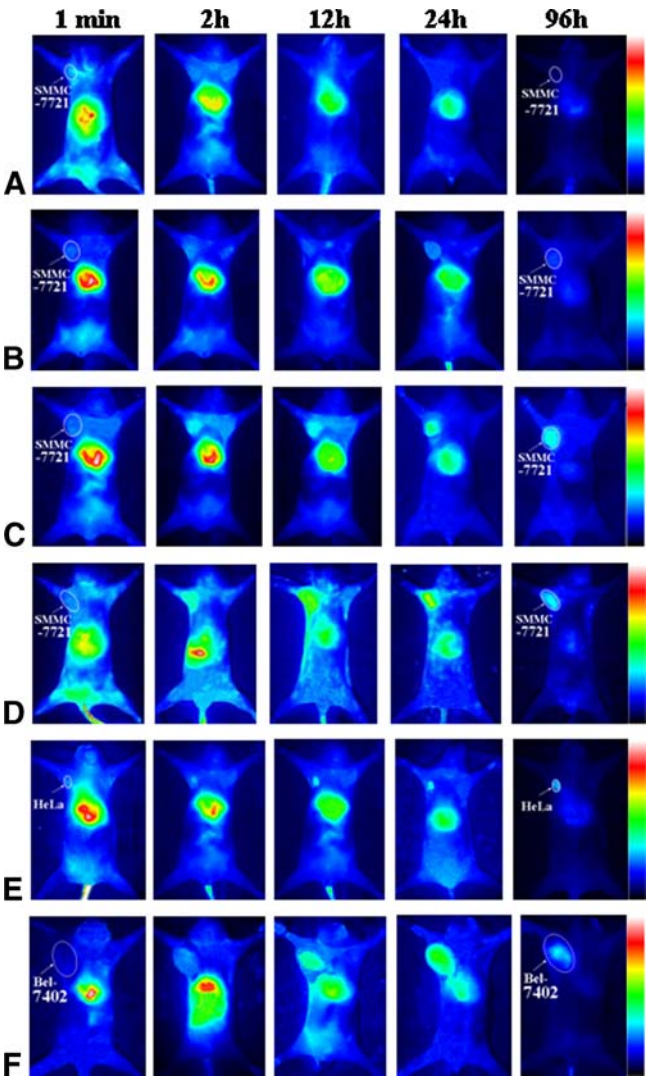

Fig. 8. *In vivo* targeting behavior of folate-NHG (dose for each group was calculated in the amount of NIRD-12.): **A** Systemic injection of free NIRD-12 (5 μg). (SMMC-7721, tumor volume: 200–400 mm^3, n=5); **B** Systemic injection of NIRD-12-loaded non-NHG (5 μg). (SMMC-7721, tumor volume: 200–400 mm^3, I=5); **C** Systemic injection of NIRD-12-loaded folate-NHG (5 μg). (SMMC-7721, tumor volume: 200–400 mm^3, n=5); **D** Systemic injection of NIRD-12-loaded D-folate-NHG (5 μg). (SMMC-7721, tumor volume: 200–400 mm^3, n=5); **E** Systemic injection of NIRD-12-loaded folate-NHG (5 μg). (HeLa, tumor volume: 30–60 mm^3, n=5); **F** Systemic injection of NIRD-12-loaded folate-NHG (5 μg). (Bel-7402, tumor volume: 600–900 mm^3, n=5).

determined by TEM. The average diameter of the magnified particles (Fig. 5C) was only about 40 nm. This may have been caused by the evaporation of water during the sample preparation of TEM, which resulted in slight shrinkage of the particles.

The optimal LC of folate-NHG for NIRD-12 is better than 1.02%, according to our previous work. In account of the accuracy of injection dose and avoiding the non-specific fluorescence of *in vivo* imaging, NIRD-12-loaded folate-NHG with LC of about 1% was prepared, and 1% of NIRD-12 in folate-NHG was enough for *in vivo* fluorescence imaging due to the good quantum yield of NIRD-12 (data not shown here) and high sensitivity of CCD camera.

NIRD-12 easily forms dimmer or multimer in aqueous solution because of its poor solubility. After being entrapped into nanohydrogel by the hydrophobic association effect, its stability will be strongly enhanced. This could be explained as the stabilization of folate-NHG for entrapped NIRD-12, which may decrease the transition energy of the chromophores of NIRD-12 and result in the occurrence of a red shift of absorption peak. The red shift of absorption peak can accordingly result in the red shift of emission peak. The interior hydrophobic microenvironment of the folate-NHG can also affect the absorption and emission peaks of NIRD-12. A similar explanation could be found elsewhere (47,48).

MTT assay implied that NIRD-12-loaded folate-NHG had little cytotoxicity, which was consistent with that of P (NIPA-co-AAm) evaluated in our previous work (36,37). The proofs of little or non-cytotoxicity of NIPA-based NHG were reported by many groups (27,43,44,49,50). Incorporation of NIPA in the backbones of polymers sometimes even reduced the cytotoxicity due to the reduction of charge density on the resulted polymer chain (50). As to NIRD-12, a derivative of indocyanine green, it is relatively safe for *in vivo* application. The low loading content (about 1%) and low leakage of NIRD-12 in the system of folate-NHG further lowers its cytotoxicity.

The targeting behavior of folate or folate-conjugate for FR expressing tumor cells was definite and extensively used as a functional ligand in tumor targeting researches (8–20). In this study, folate-NHG showed good targeting capability in all three FR positive tumor models (HeLa, SMMC-7721 and Bel-7402) with different sizes. In this *in vivo* fluorescence imaging process, D-folate-NHG showed slightly better targeting behavior than that of folate-NHG in SMMC-7721 tumor model. It indicated that more folate in folate-NHG enabled folate-NHG particles to be bound by FR with stronger adhesion and uptaken by tumor cells with higher probability.

CONCLUSIONS

FR targeting nanohydrogel folate-NHG with diameter of about 50 nm and LCST of 40°C was synthesized and characterized in this study. The photo stability of NIRD-12 was strengthened after being loaded into folate-NHG, which made it more suitable for *in vivo* real-time imaging. The active targeting behavior of folate-NHG was proved by a test of *in vivo* fluorescence imaging with the help of self-built NIR imaging system. The evaluation of the targeting and retention capability in the three tumor models demonstrated the potential application of folate-NHG in the diagnosis and therapy of different kinds of FR positive tumors. The results of FR mediated targeting test indicated that folate-NHG had obvious targeting behavior in all three FR positive tumor models with different tumor sizes after systemic administration. The accumulation of folate-NHG in tumor tissue could last for more than 96 h, which provided a promising way for FR positive tumor therapy. D-folate-NHG showed better targeting behavior than that of folate-NHG, which manifested that more folate in folate-NHG particles would be helpful for the interaction of folate and FR. More work is needed to modulate the amount of folate in folate-NHG for the best tumor targeting effect. In conclusion, folate-NHG showed promising application in tumor diagnosis and therapy. Future work will focus on the entrapment of anticancer drugs into optimal folate-NHG.

ACKNOWLEDGEMENTS

This research was funded by the Natural Science Foundation Committee of China (NSFC30371362, NSFC30672015, NSFC30700779). We thank Dr. Shuaijian Ni for MS resolution.

REFERENCES

1. Shao K, Hou Q, Duan W, Go ML, Wong KP, Li QT. Intracellular drug delivery by sulfatide-mediated liposomes to gliomas. J Control Release. 2006;115:150–7. doi:10.1016/j.jconrel.2006.07.024.
2. Hwang HY, Kim IS, Kwon IC, Kim YH. Tumor targetability and antitumor effect of docetaxel-loaded hydrophobically modified glycol chitosan nanoparticles. J Control Release. 2008;128:23–31. doi:10.1016/j.jconrel.2008.02.003.
3. Béduneau A, Saulnier P, Benoit JP. Active targeting of brain tumors using nanocarriers. Biomaterials. 2007;28:4947–67. doi:10.1016/j.biomaterials.2007.06.011.
4. Cho K, Wang X, Nie S, Chen ZG, Shin DM. Therapeutic nanoparticles for drug delivery in cancer. Clin Cancer Res. 2008;14:1310–6. doi:10.1158/1078-0432.CCR-07-1441.
5. Garanger E, Boturyn D, Dumy P. Tumor targeting with RGD peptide ligands-design of new molecular conjugates for imaging and therapy of cancers. Anticancer Agents Med Chem. 2007;7:552–8. pmid:17896915.
6. Irache JM, Salman HH, Gamazo C, Espuelas S. Mannosetargeted systems for the delivery of therapeutics. Expert Opin Drug Deliv. 2008;5:703–24. doi:10.1517/17425247.5.6.703.
7. Low PS, Henne WA, Doorneweerd DD. Discovery and development of folic-acid based receptor targeting for imaging and therapy of cancer and inflammatory disease. Acc Chem Res. 2008;41:120–9. doi:10.1021/ar7000815.
8. Salazar MDA, Ratnam M. The folate receptor: what does it promise in tissue-targeted therapeutics. Cancer Metastasis Rev. 2007;26:141–52. doi:10.1007/s10555-007-9048-0.
9. Zhao X, Li H, Lee RJ. Targeted drug delivery via folate receptors. Expert Opin Drug Deliv. 2008;5:309–19. doi:10.1517/17425247.5.3.309.
10. Yamada A, Taniguchi Y, Kawano K, Honda T, Hattori Y, Maitani Y. Design of folate-linked liposomal doxorubicin to its antitumor effect in mice. Clin Cancer Res. 2008;14:8161–8. doi:10.1158/1078-0432.CCR-08-0159.
11. Pan J, Feng SS. Targeted delivery of paclitaxel using folate-decorated poly (lactide)-vitamin E TPGS nanoparticles. Biomaterials. 2008;29:2663–72. doi:10.1016/j.biomaterials.2008.02.020.
12. Pan J, Feng SS. Targeting and imaging cancer cells by Folate-decorated, quantum dots (QDs) - loaded nanoparticles of biodegradable polymers. Biomaterials. 2009;30:1176–83. doi:10.1016/j.biomaterials.2008.10.039.

13. Okarvi SM, Jammaz IA. Preparation and *in vitro* and *in vivo* evaluation of technetium-99m-labeled folate and methotrexate conjugates as tumor imaging agents. Cancer Biother Radiopharm. 2006;21:49–60. doi:10.1089/cbr.2006.21.49.
14. Hilgenbrink AR, Low PS. Folate receptor-mediated drug targeting: from therapeutics to diagnostics. J Pharm Sci. 2005;94:2135–46. doi:10.1002/jps.20457.
15. Leamon CP, Low PS. Delivery of macromolecules into living cells: A method that exploits folate receptor endocytosis. Proc Natl Acad Sci (USA). 1991;88:5572–6. PMCID: PMC51919.
16. Müller C, Schubiger PA, Schibli R. Isostructural folate conjugates radiolabeled with the matched pair 99mTc/188Re: a potential strategy for diagnosis and therapy of folate receptor-positive tumors. Nucl Med Biol. 2007;34:595–601. doi:10.1016/j.nucmedbio.2007.05.011.
17. Sega EI, Low PS. Tumor detection using folate receptor-targeted imaging agents. Cancer Metastasis Rev. 2008;27:655–64. doi:10.1007/s10555-008-9155-6.
18. Chen WT, Mahmood U, Weissleder R, Tung CH. Arthritis imaging using a near-infrared fluorescence folate-targeted probe. Arthritis Res Ther. 2005;7:310–7. doi:10.1186/ar1483.
19. Reddy JA, Westrick E, Santhapuram HKR, Howard SJ, Miller ML, Vetzel M, *et al.* Folate receptor-specific antitumor activity of EC131, a folate-maytansinoid conjugate. Cancer Res. 2007;67:6376–82. doi:10.1158/0008-5472.CAN-06-3894.
20. Kennedy MD, Jallad KN, Lu J, Low PS, Dor BA. Evaluation of Folate Conjugate Uptake and Transport by the Choroid Plexus of Mice. Pharmaceut Res. 2003;20:714–9. doi:10.1023/A:1023421232689.
21. Leamon CP, Fei Y, Hari KS, Fan MJ, Vlahov IR. Properties Influencing the Relative Binding Affinity of Pteroate Derivatives and Drug Conjugates Thereof to the Folate Receptor. Pharmaceut Res. 2009;26:1315–23. doi:10.1007/s11095-009-9840-3.
22. Low PS, Kularatue SA. Folate-targeted therapeutic and imaging agents for cancer. Curr Opin Chem Biol. 2009;13:256–62. doi:10.1016/j.cbpa.2009.03.022.
23. Khandare J, Minko T. Polymer-drug conjugates: Progress in polymeric prodrugs. Prog Polym Sci. 2006;31:359–97. doi:10.1016/j.progpolymsci.2005.09.004.
24. Chen HY, Zhang J, Qian ZY, Liu F, Chen XY, Gu YQ. *In vivo* non-invasive optical imaging of temperature-sensitive co-polymeric nanohydrogel. Nanotechnology. 2008;19:185707–16. doi:10.1088/0957-4484/19/18/185707.
25. Chearuil FN, Corrigan OI. Thermosensitivity and release from poly N-isopropylacrylamide-polylactide copolymers. Int J Pharm. 2009;366:21–30. doi:10.1016/j.ijpharm.2008.08.036.
26. Cheng N, Liu WG, Cao ZQ, Ji WH, Liang DC, Guo G, *et al.* A study of thermoresponsive poly(N-isopropylacrylamide)/polyarginine bioconjugate non-viral transgene vectors. Biomaterials. 2006;27:4984–92. doi:10.1016/j.biomaterials.2006.05.017.
27. Mao ZW, Ma L, Yan J, Yan M, Gao CY, Shen JC. The gene transfection efficiency of thermoresponsive N, N, N-trimethyl chitosan chloride-g-poly(N-isopropylacrylamide) copolymer. Biomaterials. 2007;28:4488–500. doi:10.1016/j.biomaterials.2007.06.033.
28. Zhou YM, Ishikawa A, Okahashi R, Uchida K, Nemoto Y, Nakayama M, *et al.* Deposition transfection technology using a DNA complex with a thermoresponsive cationic star polymer. J Control release. 2007;123:239–46. doi:10.1016/j.jconrel.2007.08.026.
29. Husseini GA, Pitt WG. Micelles and nanoparticles for ultrasonic drug and gene delivery. Adv Drug Deliv Rev. 2008;60:1137–52. doi:10.1016/j.addr.2008.03.008.
30. Gu JX, Xia F, Wu Y, Qu XZ, Yang ZZ, Jiang L. Programmable delivery of hydrophilic drug using dually responsive hydrogel cages. J Control Release. 2007;117:396–402. doi:10.1016/j.jconrel.2006.11.029.
31. Carmen AL, Angel C, Alexander SD, Natalia VG, Tatiana VB, Valerij YG. Temperature-sensitive chitosan-poly(N-isopropylacrylamide) interpenetrated networks with enhanced loading capacity and controlled release properties. J Control Release. 2005;102:629–41. doi:10.1016/j.jconrel.2004.10.021.
32. Bikram M, Gobin AM, Whitmire RE, West JL. Temperature-sensitive hydrogels with SiO2-Aunanoshells for controlled drug delivery. J Control Release. 2007;123:219–27. doi:10.1016/j.jconrel.2007.08.013.
33. Wei H, Zhang XZ, Cheng C, Cheng SX, Zhuo RX. Self-assembled, thermosensitive micelles of a star block copolymer based on PMMA and PNIPAAm for controlled drug delivery. Biomaterials. 2007;28:99–107. doi:10.1016/j.biomaterials.2006.08.030.
34. Chilkoti A, Dreher MR, Meyer DE, Raucher D. Targeted drug delivery by thermally responsive polymers. Adv Drug Deliver Rev. 2002;54:613–30. doi:10.1016/S0169-409X(02)00041-8.
35. Meyer DE, Shin BC, Kong GA, Dewhirst MW, Chilkoti A. Drug targeting using thermally responsive polymers and local hyperthermia. J Control Release. 2001;74:213–24. doi:10.1016/S0168-3659(01)00319-4.
36. Zhang J, Chen HY, Xu L, Gu YQ. The targeted behavior of thermally responsive nanohydrogel evaluated by NIR system in mouse model. J Control Release. 2008;131:34–40. doi:10.1016/j.jconrel.2008.07.019.
37. Zhang J, Qian ZY, Gu YQ. *In vivo* anti-tumor efficacy of docetaxel-loaded thermally responsive nanohydrogel. Nanotechnology. 2009;20:325102–9. doi:10.1088/0957-4484/20/32/325102.
38. Kiessling F, Greschus S, Lichy MP, Bock M, Fink C, Vosseler S, *et al.* Volumetric computed tomography (VCT): a new technology for noninvasive, high-resolution monitoring of tumor angiogenesis. Nat Med. 2004;10:1133–8. doi:10.1038/nm1101.
39. Westphalen AC, Coakley FV, Qayyum A, Swanson M, Simko JP, Lu Y, *et al.* Peripheral zone prostate cancer: accuracy of different interpretative approaches with MR and MR spectroscopic imaging. Radiology. 2008;246:177–84. doi:10.1148/radiol.2453062042.
40. Weissleder R, Tung CH, Mahmood U, Bogdanov A. *In vivo* imaging of tumors with proteaseactivated near-infrared fluorescent probes. Nat Biotechnol. 1999;17:375–8. PMID: 10207887.
41. Mahmood U, Tung CH, Bogdanov A, Weissleder R. Near-infrared optical imaging of protease activity for tumor detection. Radiology. 1999;213:866–70. PMID: 10580968.
42. Destito G, Yeh R, Rae CS, Finn MG, Manchester M. Folic acid-mediated targeting of cowpea mosaic virus particles to tumor cells. Chem Biol. 2007;14:1152–62. doi:10.1016/j.chembiol.2007.08.015.
43. Cheng C, Hua W, Shi BX, Cheng H, Cao L, Gu ZW, *et al.* Biotinylated thermoresponsive micelle self-assembled from double-hydrophilic block copolymer for drug delivery and tumor target. Biomaterials. 2008;29:497–505. doi:10.1016/j.biomaterials.2007.10.004.
44. Wei H, Zhang XZ, Cheng H, Chen WQ, Cheng SX, Zhuo RX. Self-assembled thermo- and pH responsive micelles of poly(10-undecenoic acid-b-N-isopropylacrylamide) for drug delivery. J Control Release. 2006;116:266–74. doi:10.1016/j.jconrel.2006.08.018.
45. Huang G, Gao J, Hu Z, John JVS, Ponder BC, Moro D. Controlled drug release from hydrogel nanoparticle networks. J Control Release. 2004;94:303–11. doi:10.1016/j.jconrel.2003.10.007.
46. Xia XH, Hu ZB, Marquez M. Physically bonded nanoparticle networks: a novel drug delivery system. J Control Release. 2005;130:21–30. doi:10.1016/j.jconrel.2004.11.016.
47. Leobandung W, Ichikawa H, Fukumori Y, Peppas NA. Preparation of stable insulin-loaded nanospheres of poly(ethylene glycol) macromers and N-isopropylacrylamide. J Control Release. 2002;80:357–63. doi:10.1016/S0168-3659(02)00028-7.
48. Geddes CD, Cao H, Lakowicz JR. Enhanced photostability of ICG in close proximity to gold colloids. Spectrochim Acta A. 2003;59:2611–7. doi:10.1016/S1386-1425(03)00015-5.
49. Cao YX, Zhang C, Shen WB, Cheng ZH, Yu LL, Ping QN. Poly (N-isopropylacrylamide)—chitosan as thermosensitive *in situ* gel-forming system for ocular drug delivery. J Conrtol Release. 2007;120:186–94. doi:10.1016/j.jconrel.2007.05.009.
50. Turk M, Dincer S, Yulug IG, Piskin E. *In vitro* transfection of HeLa cells with temperature sensitive polycationic copolymers. J Control Release. 2004;96:325–40. doi:10.1016/j.jconrel.2004.01.013.